1 Fluorescence, its Time Dependence and Applications

It is hardly conceivable that a purchaser of this volume will not be fully conversant with molecular fluorescence in all its aspects, but for the sake of completeness, and to provide an introduction, this chapter will outline in cameo some aspects of fluorescence.

1.1 Fluorescence Intensities

Fluorescence is defined simply as the electric dipole transition from an excited electronic state to a lower state, usually the ground state, of the same multiplicity. Mathematically, the probability of an electric-dipole induced electronic transition is proportional to R_{if}^2 where R_{if}, the transition moment integral between initial state i and final state f, is given by Equation 1.1. In this equation ψ_e represents the electronic wavefunction, ψ_n the vibrational wavefunction, $\tilde{\mathbf{M}}$ is the electronic dipole moment operator, and the Born–Oppenheimer principle of separability of electronic and vibrational wavefunctions has been invoked. The first integral involves only the electronic wavefunctions of the system, and the second term, when squared, is the familiar Franck–Condon factor.

$$R_{if} = \int_{-\infty}^{+\infty} \psi_{ef} \tilde{\mathbf{M}} \psi_{ei} \, d\tau_e \int_{-\infty}^{+\infty} \psi_{nf} \psi_{ni} \, d\tau_n. \tag{1.1}$$

To a good approximation the electronic integral is zero unless the states i and f are of the same spin; hence electronic absorption in most organic molecules results in the formation of an excited singlet state from the ground singlet state. There are also symmetry restrictions on transitions between states i and f imposed by the necessity of the electronic integral being totally symmetric if it is not to become of zero value upon integration. For a transition which satisfies this requirement (symmetry allowed), the molar decadic absorption coefficient will have a maximum value of the order of 10^5 dm^3 cm^{-1} mol^{-1}. The corresponding value for the rate constant for radiative decay, k_R, of the

excited state via the spontaneous fluorescence process is given approximately by Equation 1.2, and more exactly by Equation 1.3 (Strickler and Berg, 1962).

$$k_R(s^{-1}) \simeq 10^4 \varepsilon_{max}(dm^3\,cm^{-1}\,mol^{-1}) \tag{1.2}$$

$$k_R = 2.88 \times 10^{-9} n^2 \langle \bar{\nu}_F^{-3} \rangle_{Av}^{-1} \int \varepsilon \, d\bar{\nu}/\bar{\nu} \tag{1.3}$$

where $\langle \nu_F^{-3} \rangle^{-1}$ is a measure of the average frequency of the fluorescence, $\int \varepsilon \, d\bar{\nu}/\bar{\nu}$ is the area under the absorption curve, and n is the refractive index of the medium in which the experiment is carried out. Use of Equation 1.2 for a symmetry-allowed transition gives a value of k_R of $10^9\ s^{-1}$. In the absence of any other depopulation process, therefore, the fluorescence decay time of such an excited electronic state would be $1/k_R = 10^{-9}$ s, or 1 ns. This quantity, $1/k_R$ is termed the natural or mean radiative lifetime, τ_R. In practice, because of competing processes, the actual or measured decay time, τ_F, is for complex polyatomic molecules invariably less than the mean radiative lifetime.

For a transition which does not satisfy the symmetry restrictions imposed by Equation 1.1, the transition moment integral can be non-zero if a second-order mechanism is invoked which necessitates the excitation of a vibration which is not totally symmetric in one or other of the electronic states. This has the effect of reducing the magnitude of the transition moment integral compared with that for a symmetry-allowed transition, and also leads to the absence of the absorption and emission spectral features corresponding to transitions between the vibrationless ground and excited electronic states.

In addition to symmetry restrictions on electronic transitions there are restrictions caused by the necessity of overlap in space of molecular orbitals for the electron in its initial and final states. Where this is small, for example in $n \rightarrow \pi^*$ transitions in carbonyl compounds, the electronic integral in Equation 1.1 is diminished. The "allowedness" of a transition, F, expressed as an oscillator strength, can be summarized as in Equation 1.4 by a series of factors, f, which relate in turn to spin, (s), overlap (o), p (parity), sy (symmetry), and which have the following approximate values $f_s = 10^{-5}$, $f_o = 10^{-2}$, $f_p = 10^{-1}$, $f_{sy} = 10^{-1}$ to 10^{-3}.

$$F = f_s f_o f_p f_{sy} F_A \tag{1.4}$$

F_A is the oscillator strength of a fully allowed transition. For fluorescence then ($f_s = 1$), values of k_R extend from $10^9\ s^{-1}$ for a fully allowed transition (typical say of dyestuffs), to $10^7\ s^{-1}$ for symmetry forbidden transitions (typical say of aromatic molecules), down to $10^5\ s^{-1}$ and less (for say carbonyl compounds).

It should be noted that the radiative rate constant referred to above depends upon the refractive index of the medium, n, in which it is measured. Hirayama and Phillips (1980) have reviewed the approach of several workers to the dependence of k_R upon n, and showed that all treatments lead to the

expression

$$k_R \propto n^2 \int \frac{\varepsilon(\nu)}{\nu} d\nu \tag{1.5}$$

where the integral is the area under the absorption spectrum. Controversy has arisen over the unknown dependence of this integral on n, but recent work on the substituted anthracene molecule I has shown that k_R has an overall n^2 dependence.

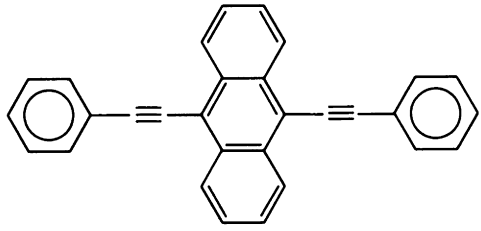

I

Table 1.1 demonstrates that for the fluorescence of the activator I, in xylene as a function of temperature, an n^2 rather than an n^3 dependence certainly gives a better fit to the observations.

Table 1.1 Dependence of τ_F for compound I upon n, n^2, n^3 in xylene

T/°C	n	τ_F/ns	$\frac{n(T)}{n(21)}\tau_F$	$\left[\frac{n(T)}{n(21)}\right]^2\tau_F$	$\left[\frac{n(T)}{n(21)}\right]^3\tau_F$
21	1.4990	3.17	3.17	3.16	3.16
39	1.4910	3.20	3.18	3.16	3.14
64	1.4785	3.27	3.22	3.17	3.13
95	1.4630	3.31	3.23	3.15	3.07
127	1.4470	3.40	3.28	3.16	3.05

The intensity of fluorescence from any excited molecule, although clearly dependent upon the magnitude of k_R as outlined above, is strongly dependent upon internal competing processes. These are shown schematically in the familiar Jablonskii diagram, Fig. 1.1. The unimolecular processes competing with fluorescence are intersystem crossing to the triplet manifold, internal conversion to the ground state, and photochemical reaction. In condensed media vibrational relaxation occurs on a picosecond timescale, and thus only chemical processes with rate constants in excess of 10^{12} s^{-1} will compete with vibrational relaxation. Subsequent to excitation therefore, vibrational relaxation is usually complete before electronic relaxation. Internal conversion is

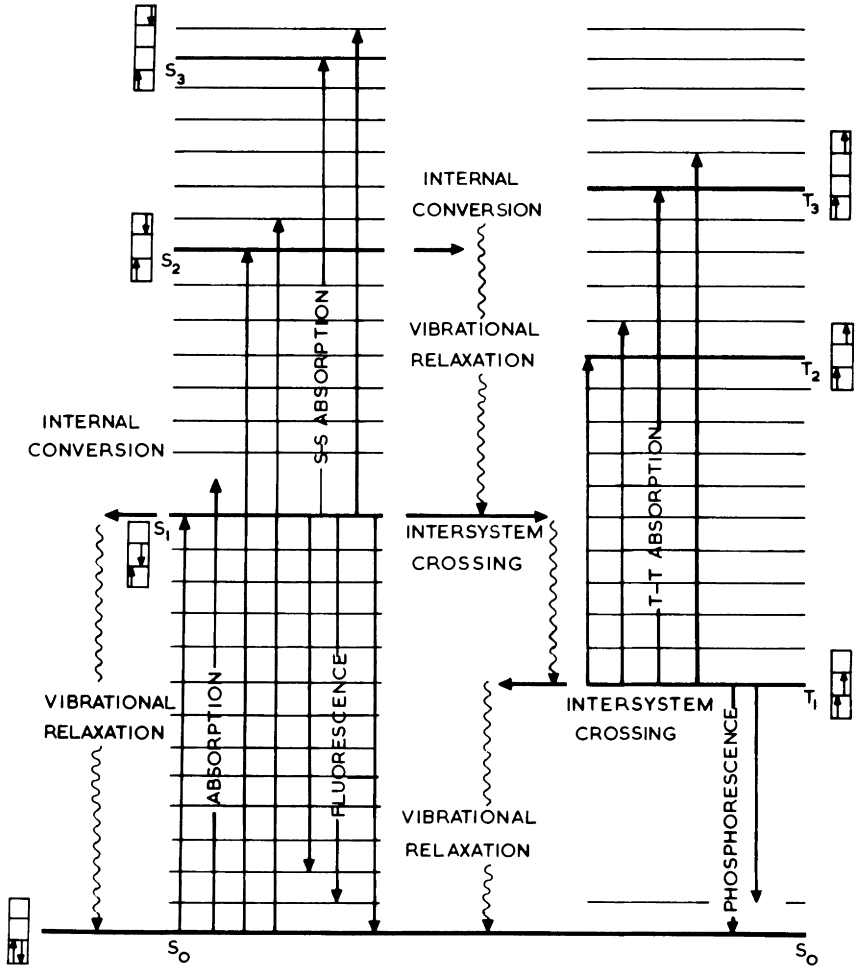

Figure 1.1 Jablonskii diagram showing fates of photoexcited complex polyatomic molecule.

usually faster at higher excess energies, but is not of great importance for lower-lying vibrational levels of the first excited singlet state. The principal process competing with fluorescence is therefore intersystem crossing to the triplet manifold of levels. Writing a simple kinetic scheme permits definition of the quantum yield of fluorescence, Φ_F, and decay time τ_F in terms of first-order rate constants (see Fig. 1.1).

	Rate constant		
$M + h\nu \rightarrow {}^1M^*$	I_a	(absorption)	(1.6)

$$^1M^* \rightarrow M + h\nu \qquad k_R \text{ (fluorescence)} \tag{1.7}$$

$$^1M^* \rightarrow {}^3M^* \qquad k_{ISC} \text{ (intersystem crossing)} \tag{1.8}$$

$$^1M^* \rightarrow M \qquad k_{IC} \text{ (internal conversion)} \tag{1.9}$$

$$^1M^* \rightarrow \text{products} \qquad k_D \text{ (dissociation)} \tag{1.10}$$

From a steady-state analysis of the scheme, the quantum yield of fluorescence Φ_F is given by

$$\Phi_F = \frac{k_R}{(k_R + k_{ISC} + k_{IC} + k_D)}. \tag{1.11}$$

The fluorescence decay time, τ_F, is given by Equation 1.12 as:

$$\tau_F = (k_R + k_{ISC} + k_{IC} + k_D)^{-1}. \tag{1.12}$$

The intensity of fluorescence seen from any molecule, even before consideration of *bimolecular* interactions, depends upon the magnitude of the rate constant k_R relative to the sum (called Σk) of k_{ISC}, k_{IC} and k_D. In some molecules, for example carbonyls, k_R is very small with respect to Σk and these molecules are thus only weakly fluorescent. Aromatic molecules, where k_R is usually of the same order of magnitude as Σk, are strongly fluorescent, and consequently very useful as probes. It is very clear from Equation 1.11 that rationalization of the photophysics and photochemistry of any singlet state molecular species in terms of the *absolute* magnitudes of rate constants for the various competing decay processes cannot be obtained with the sole knowledge of quantum yields, which are merely rate constant ratios. However, a knowledge of fluorescence decay times together with quantum yields does, in principle, provide the absolute rate information required, since

$$k_R = \frac{\Phi_F}{\tau_F} \tag{1.13}$$

$$k_{ISC} = \frac{\Phi_{ISC}}{\tau_F}, \tag{1.14}$$

and so on.

Simple decay time and quantum yield measurements have been widely used in the development of our understanding of the role of specific vibrational mode excitation in the radiative and non-radiative decay of some complex molecules. We show in Table 1.2, as an example, the fluorescence decay times and quantum yields of selected vibronic states of $^1B_{2u}(S_1)$ benzene in collision-free vapour, taken from the paper by Spears and Rice (1971). Each pair of quantum yield and lifetime values corresponds to a specific vibronic state, the identity of which has been omitted for simplicity.

Table 1.2 Lifetimes and quantum yields of single vibronic states in $^1B_{2u}$ benzene (adapted from Spears and Rice, 1971)

Energy above origin/cm^{-1}	Observed lifetime/ns	Quantum yield	Radiative lifetime/ns	Non-radiative lifetime/ns
0	100	0.22	455	128
521	79	0.27	290	108
764	77	0.26	295	104
923	83	0.21	395	105
1007	66	0.23	285	86
1042	72	0.29	250	101
1170	52	0.16	325	62
1444	71	0.21	340	90
1470	65	0.19	340	80
1547	51	0.18	285	62
1687	61	0.16	380	73
1691	52	0.24	215	68
1846	62	0.16	380	74
1930	49	0.20	245	61
1965	61	0.22	280	78
2070	55	0.06	920	59
2367	55	0.17	320	66
2393	39	0.26	150	53
2610	42	0.08	525	46
2614	42	0.06	700	45
2769	49	0.07	700	53
2888	47	0.03	1470	48

1.2 Bimolecular Interactions

In the simple kinetic scheme discussed so far bimolecular interactions other than collisional removal of vibrational energy have been neglected. Clearly in condensed media, bimolecular interactions, which may take place on a picosecond timescale, must influence the fate of the excited electronic state. The effect of the many collisions with surrounding inert medium, such as solvent, will merely be to produce a Boltzmann distribution of levels emitting fluorescence. There are, however, many specific interactions which can greatly influence the kinetics of decay. These will now be discussed briefly.

One obvious consequence of increasing the concentration of molecules M in any fluorescence experiment is to increase the probability that energy can migrate from one molecule to another by non-radiative processes, thus influencing the decay characteristics of the fluorescence:

$$^1M^* + M \rightarrow M + {}^1M^*. \tag{1.15}$$

The energy migration may occur through a series of near neighbour random hopping processes, or may occur over long distances through an induced dipole mechanism (Forster, 1946), the probability of which is given by Equation 1.16, which requires overlap of absorption spectrum of acceptor, (here M) and emission spectrum of donor (here $^1M^*$), and depends inversely on the sixth power of the distance separating the chromophores.

$$k_{ET} = \frac{K}{\tau_R R^6} \int_0^\infty f_D(\bar{\nu}) \varepsilon_A(\bar{\nu}) \, d\bar{\nu}/\bar{\nu}^4 \tag{1.16}$$

τ_R here is the mean radiative lifetime of the donor, and K is a constant given by Equation 1.17, where κ^2 is an orientation factor arising from the induced dipole nature of the transfer, which takes values between 0 and 4, a value of 2/3 being appropriate for a random distribution of molecules:

$$K = \frac{9000\kappa^2 c^4 \ln 10}{128\pi^5 n^4 N}. \tag{1.17}$$

Energy migration may reveal itself as a fast component in the decay of fluorescence of $^1M*$, being often in the picosecond region, but possibly in some synthetic polymer systems on the nanosecond timescale. It gives rise to a non-exponential form of the donor fluorescence decay law, $I(t)$, given by

$$I(t) = I(0) \exp\{-t/\tau_0 - 2B\gamma(t/\tau_0)^{1/2}\} \tag{1.18}$$

in which τ_0 is the donor fluorescence decay time in the absence of acceptor,

$\gamma = \dfrac{[A]}{[A]_0}$, the ratio of concentrations of acceptor,

$B = \left(\dfrac{1 + 10.87x + 15.5x^2}{1 + 8.743x}\right)^{\frac{3}{4}}$, where

$x = D\alpha^{-1/3} t^{2/3}$, and

$\alpha = (R^0/\tau_0)^6$ where R^0 is the value of R such that the rate of energy transfer is equal to the rate of spontaneous decay of the donor.

The interaction of an excited molecule $^1M^*$ with a ground state may in some instances lead to electronic quenching of the excited state:

$$^1M^* + M \rightarrow M + M. \tag{1.19}$$

This concentration quenching in fluid media leads to the inclusion of the term $k_M[M]$ in the expression for decay time now given by Equation 1.20. In rigid

media, where diffusional kinetics do not pertain, other models are appropriate (see for example Beavan *et al.*, 1979).

$$\tau_F^{-1} = k_R + k_{ISC} + k_{IC} + k_D + k_M[M]. \tag{1.20}$$

Inclusion of the term $k_M[M]$ yields the familiar relationship for quantum yield of fluorescence relative to that at a reference concentration,

$$\frac{(\Phi_F)_0}{\Phi_F} = 1 + k_M\tau_0[M] \tag{1.21}$$

a particular form of the Stern–Volmer relationship which here refers to self-quenching of the excited state. τ_0 in this equation is the fluorescence decay time at the reference concentration.

In many systems concentration quenching is accompanied by the appearance of a new emission band to the red of the fluorescence of the uncomplexed molecule $^1M^*$ which is attributable to the formation of an excited dimer, termed an *excimer* (Equation 1.22). Excimer fluorescence is characteristically broad, as in Fig. 1.2, and decay characteristics are complex, since excimer formation is reversible

$$^1M^* + M \rightleftharpoons {}^1(MM)^*. \tag{1.22}$$

A complete kinetic scheme is shown in Fig. 1.3, after Birks (1970). Analysis of this scheme leads to the following relationships for the decay of monomer (M) and excimer (D) fluorescence, respectively.

$$i_M(t) = A_1 \exp(-\lambda_1 t) + A_2 \exp(-\lambda_2 t) \tag{1.23}$$

$$i_D(t) = A_D[\exp(-\lambda_1 t) - \exp(-\lambda_2 t)], \tag{1.24}$$

where

$$\begin{aligned}\lambda_{1,2} = \tfrac{1}{2}\{&(k_{IM} + k_{FM} + k_{DM}[M] + k_{ID} + k_{FD} + k_{MD}) \\ &\pm [(k_{DM} + k_{FM} + k_{DM}[M] - k_{ID} - k_{FD} - k_{MD})^2 \\ &+ 4k_{DM}[M]k_{MD}]^{1/2}\}.\end{aligned} \tag{1.25}$$

The monomer decay should thus be represented by the sum of two exponential terms; that of the excimer by the difference between the same two exponential terms. These kinetics are obeyed by many simple molecular systems, but in the case of synthetic polymers, in which excimer-forming moieties are attached covalently to the backbone of, for example, a vinyl chain, the kinetics are more complex. Thus for example in a copolymer of 1-vinylnaphthalene and methylmethacrylate, the fluorescence decay of monomeric naphthalene can only be described adequately by three components. Typical data are shown in Table 1.3.

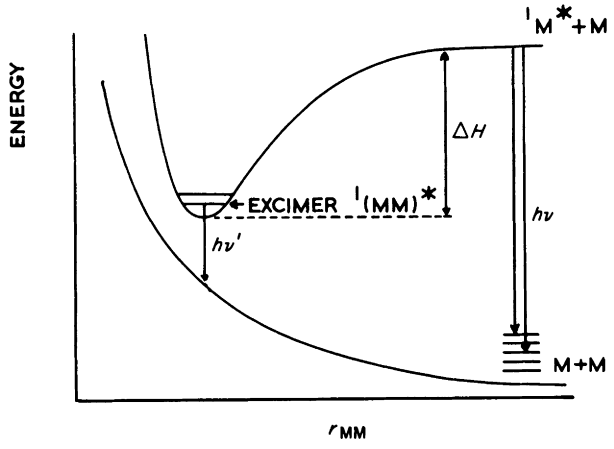

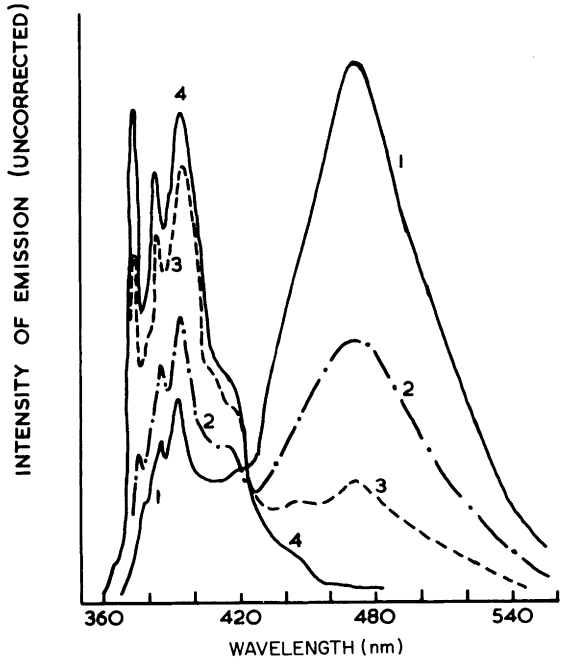

Figure 1.2 Excimer fluorescence characteristics: exaggerated potential energy diagram for excimer and resulting fluorescence spectra typified by the case of pyrene in fluid solution at concentrations (1) 3×10^{-3} M, (2) 10^{-3} M, (3) 3×10^{-4} M, (4) 2×10^{-6} M (after Parker and Hatchard, 1963).

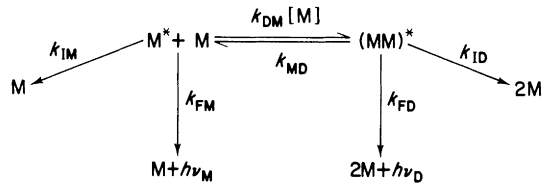

Figure 1.3 Kinetic scheme for excimer formation and decay (after Birks, 1970).

Table 1.3 Triple exponential decay data for 1-vinylnaphthalene methylmethacrylate copolymers (Roberts *et al.*, 1981)

f_n*	A_1	τ_1/ns	A_2	τ_2/ns	A_3	τ_3/ns
0.17	0.005	73.55	0.023	12.65	0.112	40.06
0.27	0.011	67.60	0.041	15.31	0.092	34.17
0.38	0.027	59.13	0.057	11.88	0.074	26.44
0.47	0.021	59.50	0.075	8.46	0.066	23.09
0.58	0.025	53.34	0.100	6.41	0.069	19.52
0.66	0.025	53.24	0.115	4.18	0.065	16.36
0.75	0.032	48.83	0.149	3.57	0.072	14.41
0.83	0.029	47.07	0.257	1.87	0.072	13.52

*f_n is mole fraction of naphthalene polymer.

Such multiple component fitting represents a somewhat hazardous exercise, with extreme care needed to ensure that parameters derived from it are meaningful, but this is now done routinely and will be described later in this volume. A rationale for the three components is given by the kinetic scheme shown in Fig. 1.4, in which two types of monomeric naphthalene are

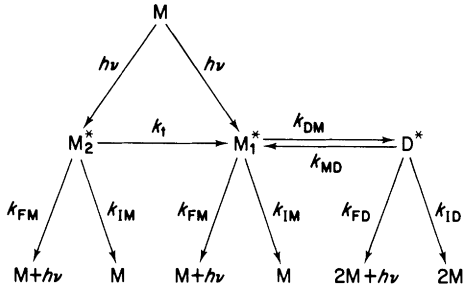

Figure 1.4 Kinetic scheme for excimer formation in vinyl aromatic polymers. In this scheme, M_1 and M_2 are two spectrally identical, but kinetically distinct monomer species, differing only in the extent to which they can participate in energy migration and thereby excimer formation.

postulated, having the same spectral distribution of fluorescence, but different kinetic behaviour. M_1 can rapidly and reversibly form excimers through energy migration and molecular motion, whereas M_2 behaves essentially as an isolated chromophore which is weakly coupled to M_1 through long range energy transfer. Such schemes are discussed widely elsewhere (see for example Roberts *et al.*, 1981).

1.2.1 Impurity quenching

In the presence of additive or impurity molecules, Q, electronically excited states may be quenched with a consequent decrease in the observed fluorescence decay time:

$$^1M^* + Q \rightarrow \text{products.} \tag{1.26}$$

Quenching may result from electronic energy transfer, often by the induced dipole mechanism referred to previously, from chemical reaction, from enhancement of non-radiative decay brought about by paramagnetic species or molecules with atoms of high nuclear charge, or by complex formation. In all cases, if the concentration of absorbing molecule M is kept constant, the Stern–Volmer relationship becomes

$$(\Phi_F)_0/\Phi_F = 1 + k_Q\tau_0[Q], \tag{1.27}$$

where $(\Phi_F)_0$ and τ_0 now refer to quantum yield and decay time of $^1M^*$ in the absence of Q. In the case of quenching by complex formation, a new fluorescence may be observed which resembles excimer fluorescence in that it is red-shifted and structureless, but is a result of charge transfer to form an excited complex (exciplex). The kinetics of this are exactly comparable to excimer kinetics.

Thus for example, the time dependence of monomer and complex concentrations, $[^1M^*](t)$ and $[^1MQ^*](t)$, are given by

$$[^1M^*](t) = -A_1e^{-\lambda_1 t} + A_2e^{-\lambda_2 t} \tag{1.28}$$

$$[^1MQ^*](t) = A_3e^{-\lambda_1 t} - A_4e^{-\lambda_2 t} \tag{1.29}$$

where the rate constants are identified in Fig. 1.5, and

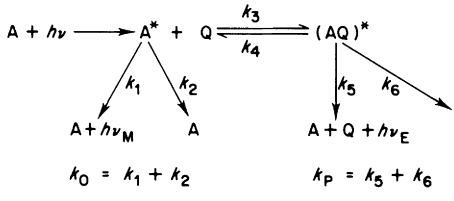

Figure 1.5 Kinetic scheme for exciplex formation.

$$A_1 = \left(\frac{k_0 + k_3[\mathrm{Q}] - \lambda_2}{\lambda_1 - \lambda_2}\right)[^1\mathrm{M}^*]_0 \tag{1.30}$$

$$A_2 = \left(\frac{\lambda_1 - (k_0 + k_3[\mathrm{Q}])}{\lambda_1 - \lambda_2}\right)[^1\mathrm{M}^*]_0 \tag{1.31}$$

$$A_3 = -A_4 = \frac{k_3[\mathrm{Q}]}{\lambda_1 - \lambda_2}[^1\mathrm{M}^*]_0 \tag{1.32}$$

and

$$\lambda_{1,2} = \tfrac{1}{2}\{k_0 + k_3[\mathrm{Q}] + k_4 + k_\mathrm{p} \pm [(k_0 + k_3[\mathrm{Q}] - k_4 - k_\mathrm{p})^2 + 4k_4k_3[\mathrm{Q}]]^{1/2}\}. \tag{1.33}$$

Equation 1.32 indicates that the A factors for the grow-in A_3 and decay A_4 of exciplex fluorescence should be of the same magnitude but opposite sign. That this relationship can be obeyed almost exactly is shown by the last two columns of Table 1.4, which contains data measured for a gas-phase exciplex system (O'Connor *et al.*, 1982).

In a few cases, weak association between a molecule M in the ground state and an additive molecule may occur.

$$\mathrm{M} + \mathrm{Q} \rightleftharpoons \mathrm{MQ} \tag{1.34}$$

Excitation of the associated complex MQ then produces an excited state ^{1}(MQ*) which may resemble closely a true exciplex. However, the kinetics of fluorescence in such a system are in principle distinguishable, since in the case of the ground-state complex excitation is instantaneous, and the complex fluorescence does not then exhibit a "growing in" period. Without giving a full analysis, in cases where such *static* quenching is of importance, measure-

Table 1.4 Fluorescence decay time data for 1-cyanonaphthalene–triethylamine exciplex in the gas phase at 188°C (O'Connor *et al.*, 1982).

	Monomer			Exciplex			
Concentration of amine $10^{-3}M$	τ_1/ns	τ_2/ns	$\frac{a_1}{(a_1+a_2)}$	τ_1/ns	τ_2/ns	a_3	a_4
0		24.1					
0.222	8.17	11.96	0.64	8.64	12.05	−0.46	0.46
0.530	5.41	10.13	0.82	5.80	11.60	−2.69	2.68
0.837	4.07	10.50	0.90	4.16	11.11	−3.68	3.70
2.13	2.00	11.23	0.98	1.96	10.97	−2.33	2.33
3.36	1.31	10.35	0.98	1.31	10.38	−1.93	1.92

ment of relative quantum yields of fluorescence $(\Phi_F)_0/\Phi_F$ and relative decay times of fluorescence, $(\tau_F)_0/\tau_F$ can be used to obtain a form of the equilibrium constant for ground-state complex formation through the following equation:

$$[(\Phi_F)_0/\Phi_F]/[(\tau_F)_0/\tau_F] = 1 + K'_{eq}[Q]. \tag{1.35}$$

Since molecular oxygen is an ubiquitous impurity, the processes by which it may quench excited states have been widely studied. Quenching of fluorescent singlet states may occur through Equations (1.36) or (1.37), with very high efficiencies.

$$^1M^* + O_2(^3\Sigma\bar{g}) \rightarrow {}^3M^* + O_2(^3\Sigma\bar{g}) \tag{1.36}$$

$$\rightarrow {}^3M^* + O_2(^1\Delta g) \tag{1.37}$$

In a heterogeneous emitting system with two (or more) fluorescence decay components, a "chemical timing" method of achieving time resolution of fluorescence spectra has been developed which depends upon the selective quenching of the longer-lived molecules by molecular oxygen.

In fluid media, the various quenching processes we have discussed, with the exception of dipole-induced dipole electronic energy transfer, yield decay curves which can be described by an exponential or a sum of exponentials. In some circumstances however, diffusional kinetics can yield an additional, observable decay term which has a $t^{-1/2}$ dependence. For a diffusion-controlled quenching reaction the continuum model predicts the fluorescence decay law to be (Nemzek and Ware, 1975)

$$I(t) = I_0 \exp(-at - 2bt^{1/2}), \tag{1.38}$$

where

$$a = 1 + 4R'D_{AQ}N'[Q] \tag{1.39}$$

and

$$b = 4(R')^2(\pi D_{AQ})^{1/2}N[Q]. \tag{1.40}$$

R' is related to the encounter distance, and D_{AQ} is the mutual diffusion coefficient of A and Q, N' is 6.023×10^{20}, and τ_0 is the decay time at $[Q] = 0$. The ratio of intensities of fluorescence under *steady* illumination is predicted to be

$$(I_0/I) = [1 + 4R'D_{AQ}N'[Q]\tau_0]Y^{-1}, \tag{1.41}$$

where

$$Y = 1 - (b/a^{1/2})\pi^{1/2}\exp(b^2/a)\mathrm{erfc}(b/a^{1/2}) \tag{1.42}$$

and

$$\text{erfc}(x) = 2\pi^{-1/2} \int_x^\infty \exp(-u^2)\,du. \tag{1.43}$$

That the decay law is indeed represented by Equation 1.38 is established in Fig. 1.6 for the quenching of 1,2-benzanthracene by CBr_4 (Nemzek and Ware, 1975). However, a test of the consistency of the model is to deconvolve decay curves according to Equation 1.38, use resulting values of a and b to compute R' and D, and *calculate* values of $(I_0)/I$. These can then be compared with experiment. However in no case reported to date is there good agreement, and a large contribution of static quenching is thus invoked to explain the observed results (see for example Nemzek and Ware, 1975; Beddard *et al.*, 1978).

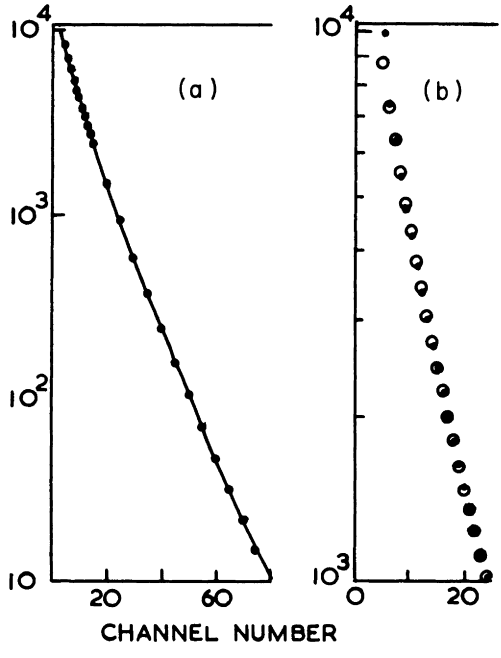

Figure 1.6 Experimental data (a: line, b: open circles) for decay of 1,2-benzanthracene fluorescence quenched by CBr_4 and computed decay (filled circles) for $I(t)$ using Equation 1.38 (from Nemzek and Ware, 1975). (a) Three decades; (b) one decade decay.

1.3 General Environmental Effects

There are effects other than specific electronic quenching effects which may influence the time-resolved behaviour of fluorescence of molecules. We have already discussed the effect of refractive index upon the radiative rate constant, but there are general dielectric effects of the medium which are responsible for *spectral* shifts, and which may also influence the nature of the emitting state, and hence its decay characteristics.

The spectral distribution of fluorescence is dictated by the Franck–Condon factors defined as the square of the second term in Equation 1.1 and the position of the centre of gravity of the fluorescence depends upon any geometry changes between ground and excited states. The latter point is illustrated in Fig. 1.7 from which it can be seen that the most probable transition in absorption is to higher energies than that for fluorescence if the potential surface of the excited state undergoes some non-zero displacement with respect to the ground state, and assuming that vibrational relaxation is complete prior to electronic relaxation. If vibrational relaxation is incomplete, then a time-dependent fluorescence spectrum results. However, since in condensed media vibrational relaxation occurs on a picosecond timescale, time-dependent spectra due to this phenomenon can only be observed in picosecond experiments. Solvent relaxation occurs on a longer timescale, and can result in the observation of nanosecond time-resolved spectra.

The spectral position of absorption and fluorescence is influenced by the dielectric properties of the medium in which observations are made. Figure 1.8 shows that the vapour phase O–O bands in absorption and fluorescence of a molecule are identical, whereas in solution with solvent of static dielectric constant ε and refractive index n, the bands are no longer coincident. The differences can be rationalized as follows. From Onsager theory, a solute molecule of dipole moment μ in a spherical cavity of radius a polarizes the dielectric of the solvent, producing a reaction field. This field, R_0, is given for the ground state of the solvent molecule (of dipole moment μ_0), by:

$$R_0 = \frac{2\mu_0(\varepsilon - 1)}{a^3(2\varepsilon + 1)} \tag{1.44}$$

Upon excitation, and invoking the Franck-Condon principle, the electronic excitation is much more rapid than the dielectric relaxation time of the solvent, so the reaction field of the Franck–Condon excited state R_1' is given by Equation 1.45, in which the solvent still experiences the ground state solvent dipole moment, and the high frequency dielectric constant ($=n^2$) is used in place of ε:

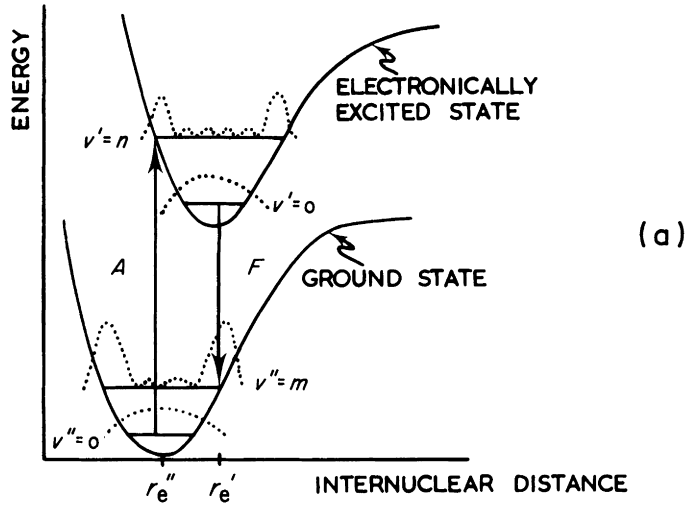

STOKES LOSS = (A-F)/2

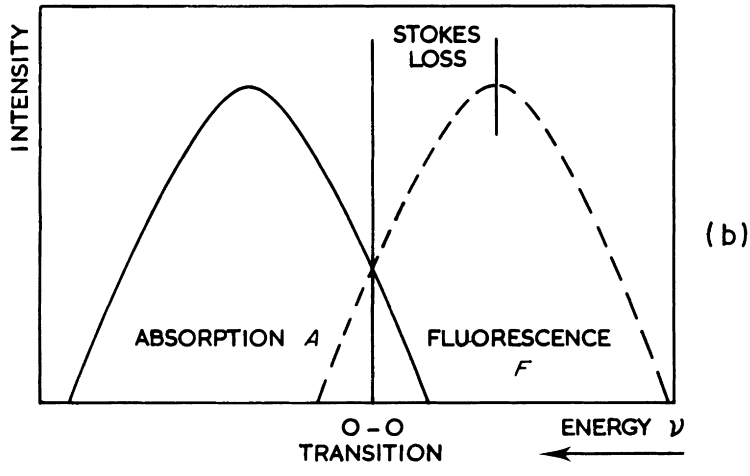

Figure 1.7 Stoke's loss. (a) Potential energy surfaces for pseudo-diatomic molecule showing most probable transitions. (b) Resulting absorption and emission spectra. (No vibrational structure is shown, although this can be encountered in many polyatomic molecules.)

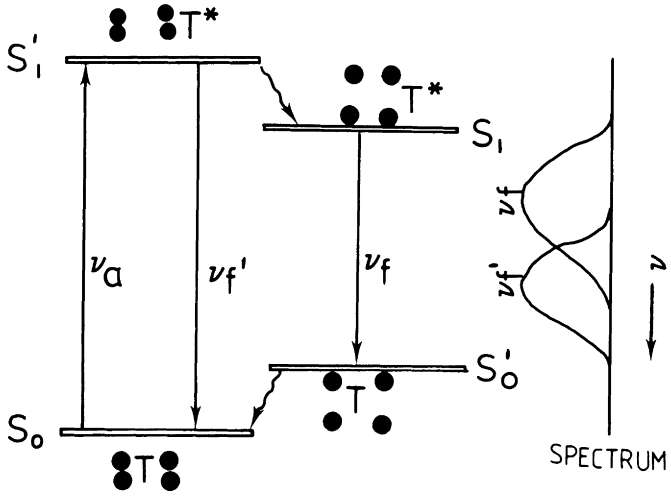

Figure 1.8 Schematic of solvent relaxation, with resulting fluorescence spectral shift for solute molecule T.

$$R_1' = \frac{2\mu_0}{a^3}\frac{(n^2-1)}{(2n^2+1)}. \tag{1.45}$$

If the decay time of the excited state of the solvent exceeds the dielectric relaxation time, then the equilibrated excited state system of dipole moment μ', has a reaction field given by:

$$R_1 = \frac{2\mu'}{a^3}\frac{(\varepsilon-1)}{(2\varepsilon+1)}. \tag{1.46}$$

Following fluorescence, the non-equilibrium ground state has a reaction field R_0', given by:

$$R_0' = \frac{2\mu'}{a^3}\frac{(n^2-1)}{(2n^2+1)} \tag{1.47}$$

Manipulation of these equations shows that the difference in energy of the O–O transitions in absorption and emission is given by Equation 1.48.

$$\Delta\bar{\nu} = \frac{2(\mu'-\mu_0)^2}{hca^3}\left[\frac{(\varepsilon-1)}{(2\varepsilon+1)} - \frac{(n^2-1)}{(2n^2+1)}\right]. \tag{1.48}$$

For non-polar solvents $\varepsilon \simeq n^2$, and no shifts are observed. For polar solvents shifts can be large. Therefore fluorescence spectral position can be very sensitive to the environment of the fluorescent molecule, and such obser-

vations are for example widely used in biological studies to identify different sites in heterogeneous systems such as cell membranes. Where solvent relaxation is slow compared to the decay time of the fluorescent molecule, time-dependent fluorescence spectra will be observed. For example, it is shown in Fig. 1.9 that the time-resolved (gated) spectra of the toluidino-naphthalene sulphonate (TNS) molecule (much used as a probe in biological membranes) are markedly dependent upon the time elapsing after excitation, clearly demonstrating the timescale of solvent relaxation.

Due to the nature of some excited and ground states, *specific* solvent effects may sometimes be observed. For example in states arising from $n \rightarrow \pi^*$ excitations, the absorption bands undergo blue shifts in polar solvents relative to those observed in non-polar solvents, due to the binding of the non-bonding electrons to the solvent. Where there are two excited states of differing electronic configuration in close proximity, change of solvent polarity can invert the ordering of the excited states, leading to a change in the nature of the fluorescence, which can clearly influence spectral profile, decay time and yield. In mixed solvents, or in heterogeneous systems, level inversion can lead to time-dependent spectra, and complex fluorescence decays.

An example is the aminonaphthalene molecule, widely used as the basic chromophore of many probes in biochemistry, for which time-resolved spectra are shown in Fig. 1.10 (Meech *et al.*, 1983). Results can only be

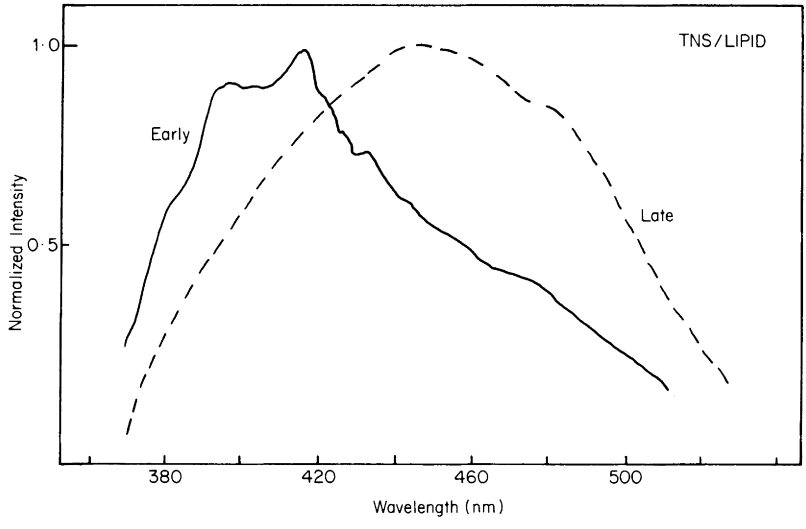

Figure 1.9 Time-resolved spectra of the probe molecule TNS (see text) in a lipid bilayer of egg phosphatidylcholine. Early spectrum at $t = 0$ gate width 2.5 ns, late spectrum at $t = 31$ ns, gate width = 2.5 ns (after Phillips *et al.*, 1979).

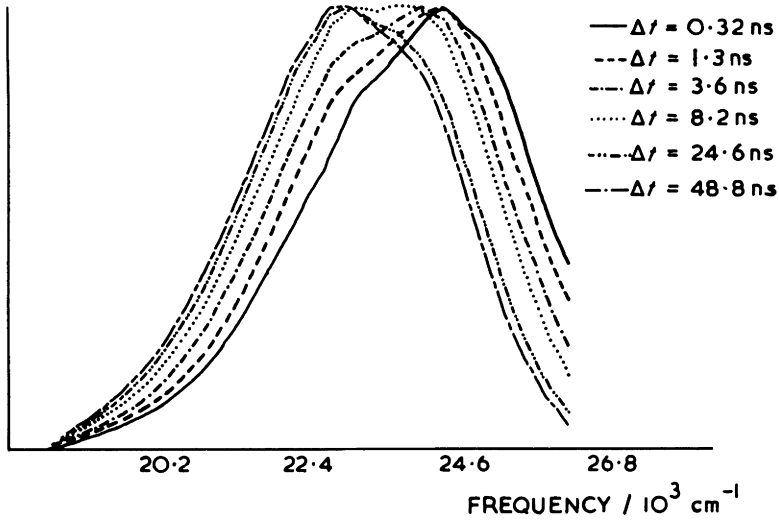

Figure 1.10 Time-resolved spectra of amino-naphthalene in butanol at 190 K. "Gated" spectra taken after delays shown (after Meech *et al.*, 1983).

interpreted in terms of two relaxation mechanisms, one an intramolecular electronic reorganization, increasing the charge-transfer nature of the emitting state in polar media (see Fig. 1.11), and the second, a *solvent* dipole relaxation about the excited state dipole moment. The relative positions of the lowest two states of this chromophore as a function of solvent, time and viscosity are summarized in Fig. 1.11 (Meech, 1983). That such a complex system should yield non-exponential fluorescence decays is not perhaps surprising.

It must not be forgotten that the viscosity of the medium can play a role in determining decay characteristics. In the case of anthracene and 9-methylanthracence, for instance, which exhibit only small spectral changes in hydrocarbon solvents of varying viscosity, measured decay times vary as shown in Figs 1.12 and 1.13 (Blatt *et al.*, 1981). The dependence in each case is different, but pronounced, and is attributable to different viscosity dependences of Franck–Condon factors for non-radiative decay of the molecules.

As a further specific example of solvent effects upon measured decay times, we can cite one example of the very widely met problem of acid–base equilibria in β-carboline (Sakurovs and Ghiggino, 1982). Various acid–base equilibria, as shown in Fig. 1.14, are possible. The measured total fluorescence decay times vary from $\tau = 22.0$ ns at pH = 3.6 to $\tau = 1.60$ ns at pH = 14 corresponding to emission from the cation, $\lambda_{max} \sim 450$ nm at pH = 3.6 to

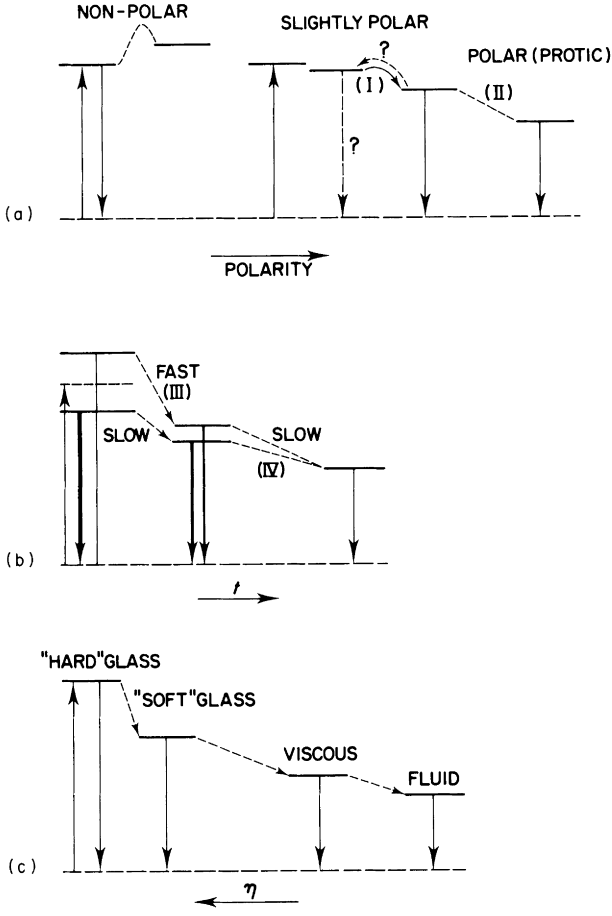

Figure 1.11 State diagrams for aminonaphthalene in solvents as function of (a) solvent, (b) time, and (c) viscosity (after Meech *et al.*, 1983).

that from the Zwitterion, $\lambda_{max} = 510$ nm at pH = 14. Clearly in such complex systems identification of emitting species must be approached with care.

1.4 Polarization of Electronic Transitions

The transition dipole moment operator $\tilde{\mathbf{M}}$ contained in Equation 1.1 is a vector quantity; in other words the change in position of the electron in the transition is in a fixed direction with respect to some system of coordinates in which the molecular frame is fixed. The dipole moment operator is resolvable

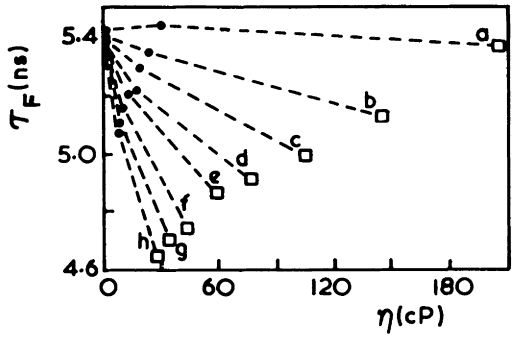

Figure 1.12 Viscosity dependence of fluorescence decay time of anthracene in hexane. ●, oil A; and □, oil B at (a) 20°C, (b) 25°C, (c) 30°C, (d) 35°C, (e) 40°C, (f) 45°C, (g) 50°C and (h) 55°C. [Reprinted with permission from Blatt *et al.* (1981). Copyright 1981 American Chemical Society.]

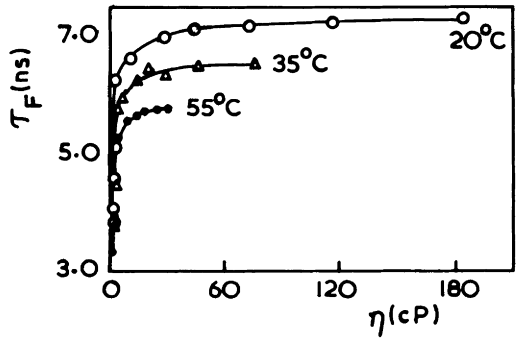

Figure 1.13 Viscosity dependence of 9-methylanthracene fluorescence decay times. [Reprinted with permission from Blatt *et al.* (1981). Copyright 1981 American Chemical Society.]

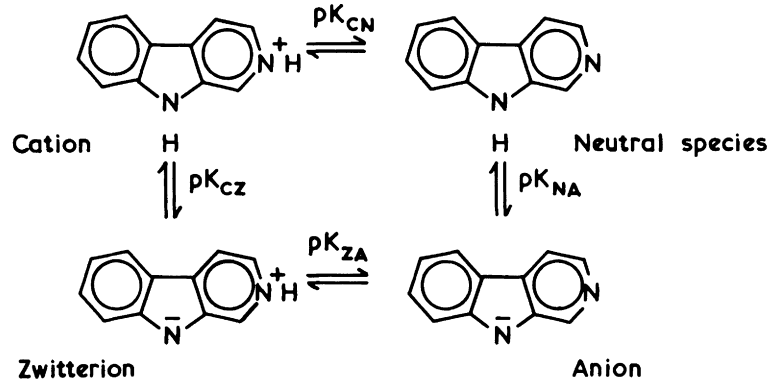

Figure 1.14 Acid–base equilibria and pKa's for B-carboline (after Sakurovs *et al.*, 1982).

in three directions such that, for any transition, only one component will be finite.

$$\hat{\mathbf{M}}^2 = \hat{\mathbf{M}}_x^2 + \hat{\mathbf{M}}_y^2 + \hat{\mathbf{M}}_z^2 \tag{1.49}$$

Hence if a perfectly ordered system such as a fixed molecular single crystal absorbs plane-polarized light, there will generally be one orientation of the crystal axes with respect to the plane of the polarization which maximizes the absorption probability. Normally fluorescence involves the transition between the same two states as are observed in absorption (i.e., the light emitted as the same directional properties with respect to the electric vector as has the light absorbed).

In two-dimensional representation the fluorescence intensity component parallel to the plane of polarization of the electric vector of the incident radiation (the reference direction), $I_{||}$ and that perpendicular to the reference direction $I_{\perp}$ varies with θ, the angle between the reference direction and direction of the optical transition moment on a laboratory scale, since the molecule is rigid. The exact magnitude of $I_{||}$ and $I_{\perp}$ as a function of θ can be traced out in the circular diagram shown in Fig. 1.15.

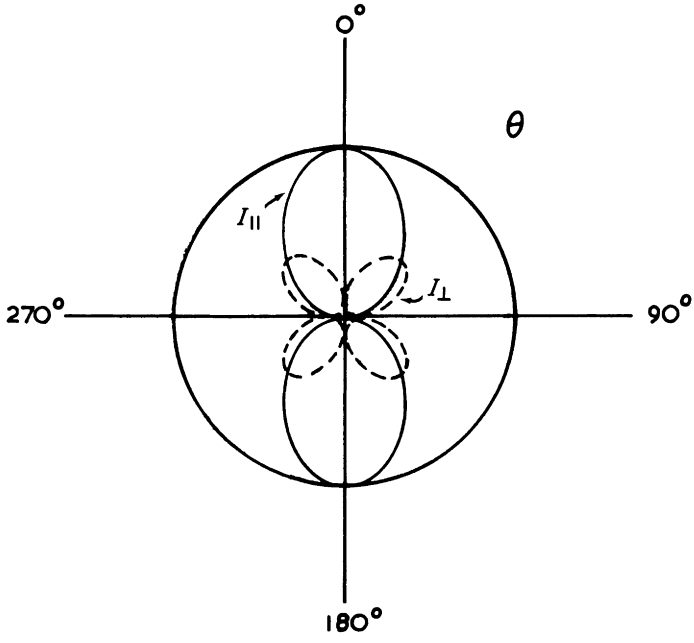

Figure 1.15 Traces of relative values of $I_{||}$ and $I_{\perp}$ for single fixed chromophore rotated through angle θ with respect to vertically polarized exciting light. At $\theta = 0$, transition moment is parallel to the plane of exciting light.

It should be noted that this diagram has been constructed for a fixed single molecule, but is clearly also appropriate for a perfectly ordered fixed system with transition moments of all absorbing chromophores parallel. If, as usual, the degree of polarization P is defined as

$$P = \frac{I_{||} - I_{\perp}}{I_{||} + I_{\perp}}, \tag{1.50}$$

it can be seen that it will vary with θ for this system between the limits of $+1$ and -1 between $\theta = 0$ and $\theta \to 90°$. For a perfectly random array of absorbing chromophores, it is easily shown that for a parallel (fluorescent) emission, P has the value of $+0.5$ independent of θ, whereas for a perpendicular transition, $P = -0.33$.

In fluid media, this analysis is only appropriate if the average rotational relaxation time τ_r is very long compared with the fluorescence decay time, τ_F, ($\tau_r \gg \tau_F$). If the opposite is true, i.e., $\tau_F \gg \tau_r$, all anisotropy introduced in the sample upon excitation is lost through the rotational relaxation prior to emission. If τ_r and τ_F are comparable, then partial relaxation will occur on the same timescale as emission of fluorescence, and analysis of the time-dependence of the fluorescence anisotropy can yield information concerning the rotational motion. The emission anisotropy r is defined as

$$r(t) = \frac{I_{||}(t) - I_{\perp}(t)}{I_{||}(t) + 2I_{\perp}(t)} \tag{1.51}$$

and at time zero, r_0 is given by

$$r_0 = \frac{1}{5}(3\cos^2\delta - 1), \tag{1.52}$$

where δ is the angle between absorption and emission dipoles, which for fluorescence, is usually zero. In general,

$$r(t) = r_0 M_2(t) = r_0 \frac{\langle 3\cos^2\theta(t) - 1\rangle}{2}, \tag{1.53}$$

where $M_2(t)$ is the orientation autocorrelation function, and $\theta(t)$ the angle through which the emission transition moment turns between time zero and t.

For a rigid sphere, Einstein showed that $r(t)$ is a single exponential function.

$$r(t) = r_0 e^{-6Dt}, \tag{1.54}$$

where D is the rotational diffusion coefficient.

The time-averaged value of $r(t)$ is

$$\bar{r} = \frac{\int_0^\infty r(t)I(t)\,dt}{\int_0^\infty I(t)\,dt}. \tag{1.55}$$

This leads to the Perrin relationship:

$$\frac{1}{r} = \frac{1}{r_0}\left(1 + \frac{3\tau_F}{\tau_r}\right), \tag{1.56}$$

or, expressed in terms of degree of polarization:

$$\left(\frac{1}{P} - \frac{1}{3}\right) = \left(\frac{1}{P_0} - \frac{1}{3}\right)\left(1 + \frac{3\tau_F}{\tau_r}\right). \tag{1.57}$$

Therefore if the decay time τ_F of a probe molecule is known, a measure of the single rotational relaxation parameter τ_r can be made if the time averaged degree of polarization is measured (using continuous excitation), and P_0 is known. In practice P_0 is not known, and use is made of the relationship $\tau_r = 3V\eta/kT$ where η is the viscosity of the medium. Measurement of P in solvents of different viscosity then permits evaluation of V and P_0. A typical result of such an experiment is shown in Fig. 1.16, for a copolymer system tagged with anthracene.

There are, however, many uncertainties in the procedure, and it seems clear that direct measurement of the time dependence of emission anisotropy through $I_{||}(t)$ and $I_{\perp}(t)$ is preferable, particularly since the general form of $r(t)$ will only rarely conform to a single exponential component. This area is discussed fully in Chapter 8 of this volume, but a simple example is shown in Fig. 1.17 of measurement of $I_{||}(t)$ and $I_{\perp}(t)$, from which $r(t)$ can be constructed through Equation 1.51. Unusually, in this case, $r(t)$ is not strongly time-

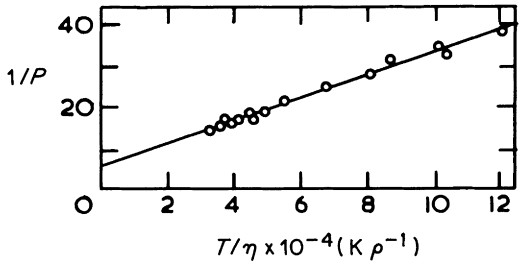

Figure 1.16 Perrin plot of reciprocal fluorescence polarization against T/η for a copolymer (P-chlorostyrene-9-vinylanthracene) in toluene, where P is the degree of polarization T is the temperature in degrees Kelvin, and η is the viscosity of the medium (after North and Soutar, 1972).

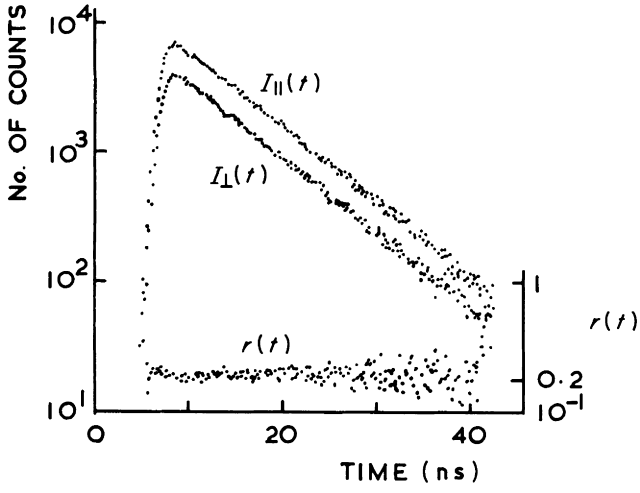

Figure 1.17 Parallel ($I_{\parallel}(t)$) and perpendicular ($I_{\perp}(t)$) polarized components of the fluorescence decay for DPH dispersed in a nematic liquid crystal. The emission anisotropy $r(t)$ is also shown (after Palmer *et al.*, 1974).

dependent, indicating the substantial order in the system under study, a nematic liquid crystal, and the lack of freedom of motion of the probe.

1.5 Measurement of Fluorescence Decay Times

The preceding discussion will have served, it is hoped, to illustrate some of the many needs for accurate measurement of fluorescence decay times. We shall now outline briefly methods available for such measurement.

1.5.1 Modulation methods

The first method employed directly for the measurement of decay times was that of phase-modulation, described as long as fifty years ago. In this technique, a sample is excited by a light source, modulated (usually sinusoidally) at between 10 and 50 MHz, and reliance is placed upon the measurement of the phase angle between detected fluorescence and the exciting light, δ, and the amplitude of the modulated signal. Such a system is illustrated in Fig. 1.18, shown for use in measuring polarized components of fluorescence. For an exponentially decaying signal, the relationship between δ, and the modulation frequency, ν, is

$$\tan \delta = 2\pi\nu\tau. \tag{1.58}$$

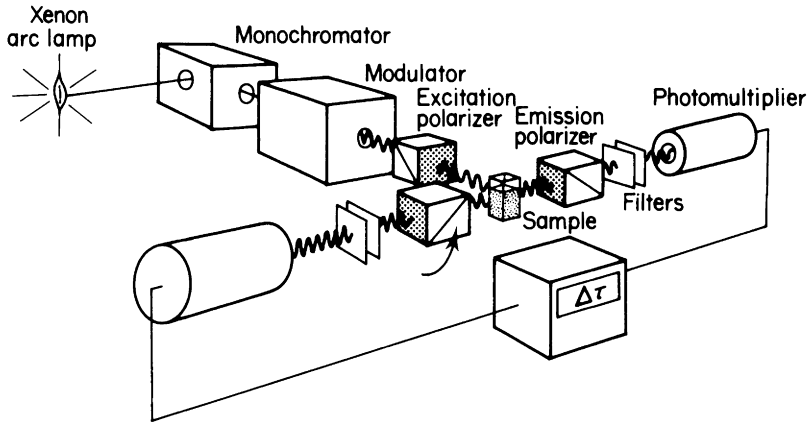

Figure 1.18 Schematic diagram of phase-modulation fluorimeter, used in this arrangement for anisotropy measurements (after Cossins, 1981).

This deceptively simple expression forms the basis of commercial instruments, such as that manufactured by SLM Inc., and the method has gained a considerable number of users. Its drawbacks include the stringent requirement that spurious modulations be excluded, and the fact that, until recently, analysis for anything other than a single component was almost impossible. However, there have been some remarkable improvements recently, which render the analysis of multiple components much more simple, and also permit the recording of time-resolved fluorescence spectra. We refer the reader to a system developed by Gugger and Calzaferri (1980), based upon laser excitation, which is capable of high resolution, and in which decay times as short as 10 ps could in principle be measured. The apparatus is shown in Fig. 1.19, and is essentially a dual beam instrument of high resolution. It may well be that in future years more reliance will be placed upon such phase-modulation techniques, but at present, it seems that pulsed techniques still command the loyalty of the majority of users.

A method related to phase-modulation has been used to demonstrate that lifetimes as short as 200 ps can be measured using the mode noise in a free running argon ion laser to produce variations in the excited state population of a fluorophore. Measurement of the r.f. power spectrum of the resulting fluctuations yield the excited state lifetime. Mode noise contains very high frequency fluctuations which the excited state population cannot follow because of its finite lifetime, and therefore these components will be absent from the r.f. spectrum of the fluorescence fluctuations. The fluorescence process thus acts like a low-pass exponential filter, and comparison of the

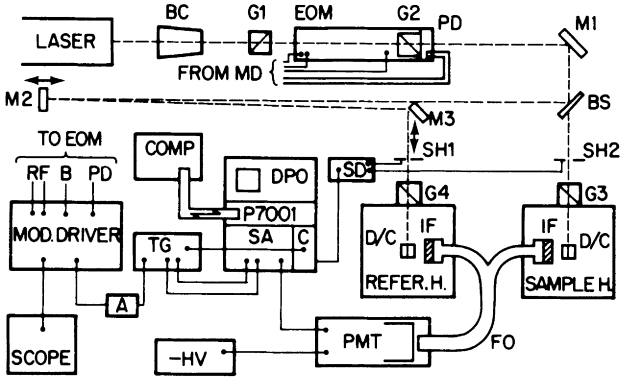

Figure 1.19 Experimental layout for laser-excited modulation experiment for fluorescence decays (after Gugger and Calzaferri, 1980). ---, laser beam; ○———○, electrical connections. Optics: BC, beam collimator; G1–G4, Glan prism polarizers; M1–M3, mirrors; BS, beam splitter; IF, interference filter; FO, fibre optics. Electronics: DPO, digital processing oscilloscope; P7001, processor of the DPO; COMP, minicomputer; SA, spectrum analyser plug in; C, counter plug in; TG, tracking generator; A, amplifier; SD, shutter driver; PMT, photomultiplier; HV, high voltage supply. Modulator: EOM, electro-optical modulator; PD, photodiode assembly; MD, modulator driver; RF, output and termination of r.f. driving voltage; B, bias voltage. Housings: REFER. H., reference chamber; SAMPLE H., sample chamber; D/C, diffuser or cuvette.

fluorescence power spectrum with that of the source provides the decay time data, as the following treatment demonstrates.

For a fluorophore, the intensity decaying exponentially as in Equation 1.59 has a spectral power density in the frequency domain

$$I(t) = I_0 \exp(-t/\tau), \tag{1.59}$$

found by Fourier transformation to be

$$P_F(\omega) = \tau^2/(1 + \tau^2\omega^2). \tag{1.60}$$

The frequency-domain signal is measured in this case at the discrete frequencies at which laser mode beats occur. The time domain representation of these beat frequencies is

$$A(t) = \sum_n A_n \cos(\omega_n t), \tag{1.61}$$

where A_n is the amplitude of the beat at frequency ω_n. Fourier transformation of this yields

$$P_s(\omega) = \sum_n A_n \delta(\omega - 2\pi f_0 n). \tag{1.62}$$

The observed noise spectrum of a fluorescence signal excited by a laser with the beat frequency pattern of Equation 1.61 is then the product of Equations 1.60 and 1.62, or

$$P'_{\mathrm{F}}(\omega) = \sum_n A_n^2 \tau^2 \delta(\omega - 2\pi f_0 n)(1 + \omega^2\tau^2)^{-1}. \tag{1.63}$$

The time-averaged beat frequency of a laser is stable over long periods of time, so that it is possible to obtain a spectrum (from scatter) proportional to Equation 1.62 (Fig. 1.20(a)). Division of the observed fluorescence fluctuation spectrum of Fig. 1.20(b) by such a pattern yields the frequency domain lifetime directly through Equation 1.63. This is shown for Rhodamine B in Fig. 1.21 to yield a decay time of 3.2 ns.

There are limits on this method which are imposed by the large spacing of

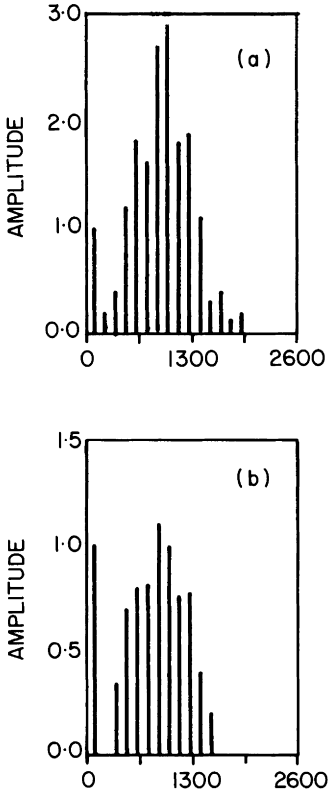

Figure 1.20 Time-resolved power spectrum of (a) fluctuations in scattered radiation and (b) fluctuations in fluorescence of Rhodamine B, normalized to the 130 MHz beat of the exciting Ar^+ in laser (after Hieftje *et al.*, 1977).

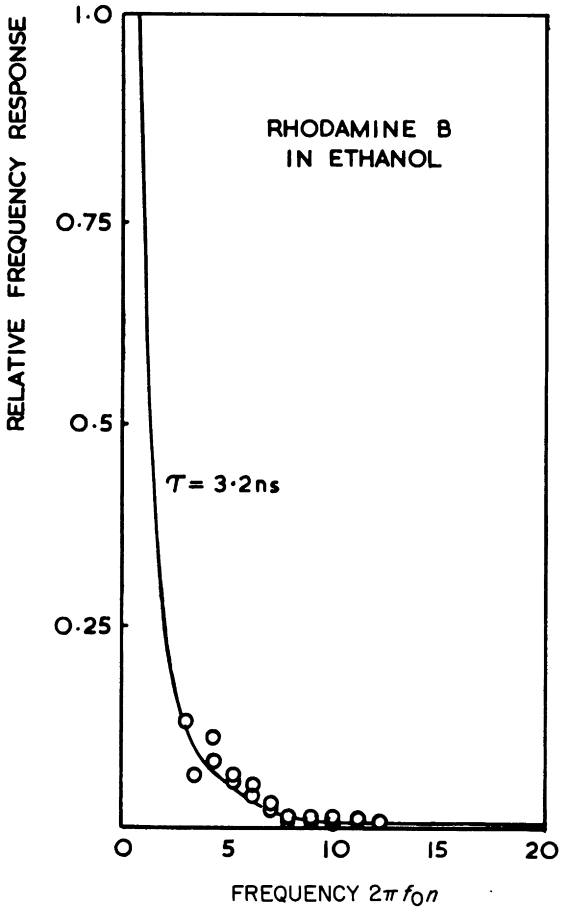

Figure 1.21 Frequency response of fluorophore Rhodamine B normalized at the first beat frequency (after Hieftje *et al.*, 1977).

laser mode-noise peaks (130 MHz), setting an upper decay time limit of 7 ns, by detector noise background setting a lower limit of 200 ps, of cost (of a spectrum analyser) and of difficulties in analysis of multicomponent fluorescence. However, as any source could in principle be used to measure a noise spectrum, the method is worth further consideration.

1.5.2 Pulse-sampling methods

Early techniques for fluorescence decay measurements used a gaseous discharge lamp, of a few nanoseconds duration to excite the sample, and

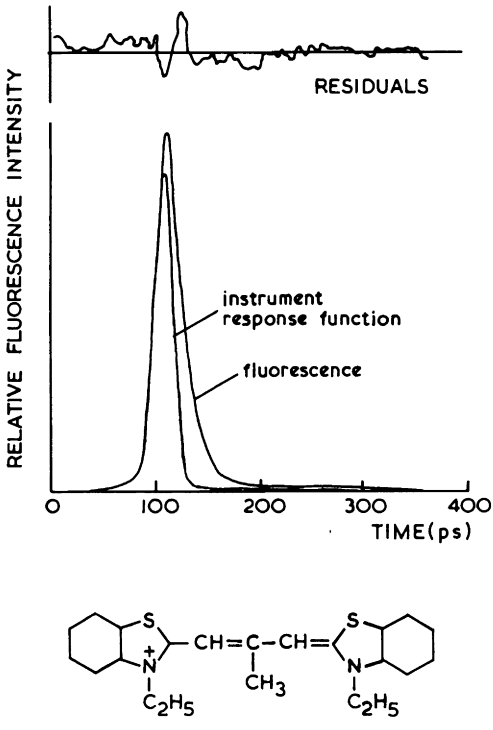

Figure 1.22 Fluorescence decay of dye shown measured by the second harmonic of Nd^{3+} laser excitation, using streak camera detection (from Winkworth *et al.*, 1982).

detected fluorescence was monitored by a photomultiplier for direct display on a fast sampling oscilloscope (Meserve, 1971; North and Soutar, 1972). Although simple, the technique is insensitive, and prone to difficulties when attempts are made to measure decay times below about 10 ns. A more recent and elegant extension of the technique is to use mode-locked picosecond solid-state lasers for excitation with streak-camera detection of fluorescence. With these methods, decay times from 10 ps to, perhaps, 1 ns can be measured, and Fig. 1.22 shows a typical decay.

Although very high temporal resolution is possible, the apparatus is costly, the range limited, and measurements are still far from routine. The advent of a new generation of synchroscanning streak cameras, while not diminishing the costs of these measurements, promises to make experimental techniques easier, and to render accessible both longer and shorter timescales, particularly the latter when used in conjunction with sub-picosecond mode-locked dye laser systems for excitation.

1.5.3 Time-correlated single photon counting

The first use of a time-to-amplitude converter as an approach to the measurement of fluorescence decay seems to have been that of Koechlin (1961). By the 1970s, single photon counting had become standard practice although refinements continue to this day. The method has been the subject of a number of reviews, those of Ware (1971), Yguerabide (1972), Poultney (1972), Knight and Selinger (1973), Isenberg (1975), Badea and Brand (1979), and Birks and Munro (1967) being especially worthy of note. Since the remainder of this volume is concerned exclusively with the technique, no further discussion will be given here.

1.5.4 Pump and probe techniques

The ultimate time resolution of streak cameras may be sub-picosecond, and they thus represent a costly but effective means of detection of very fast decays. Phase-modulation methods may ultimately be used down to about 10 ps, although at present detection limits for reliable measurements are rather longer. Time-correlated single photon counting, being based upon a photomultiplier detection, has a limit perhaps of about 20 ps (Ghiggino *et al.*, 1980).

Improvements over this may be achieved using laser excitation in some pump and probe configuration. An original early example of this technique is shown in Fig. 1.23. Here fluorescence is excited by the second, or fourth

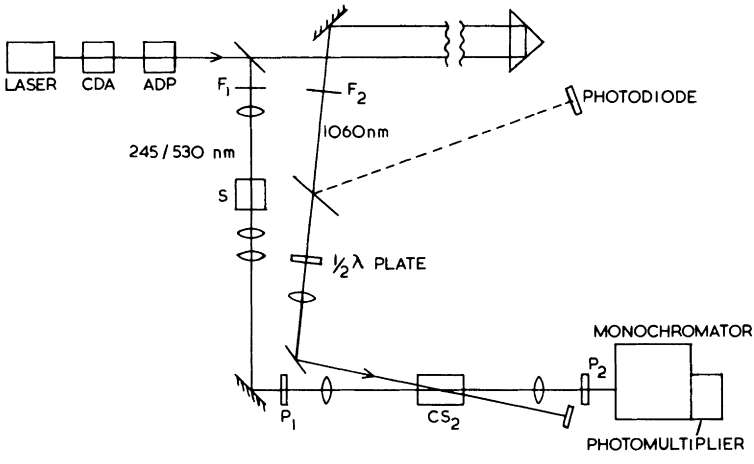

Figure 1.23 Laser arrangement for picosecond measurements of fluorescence decay using CS_2 shutter (Porter *et al.*, 1974).

harmonic of a neodymium in glass laser, and a Kerr cell shutter, (CS_2 solution) is opened by a delayed fundamental pulse from the same laser. Timing is thus achieved by the delay of the interrogating pulse, and this can be achieved accurately, the monochromator and photomultiplier combination being used solely to monitor total intensity at the time the shutter is opened. The Kerr effect consists of rotation of the plane of polarization of light through 90° in the presence of a high electric field. In this experiment, the laser fundamental is of sufficient intensity to achieve this, and by placing the Kerr cell between crossed polarizers, the shutter can be made to operate.

A recent very elegant pump and probe method termed up-conversion has been devised which permits picosecond fluorescence decay and anisotropy measurements to be made. Up-conversion refers to "the non-linear phenomenon of sum-frequency generation in anisotropic crystals", and the apparatus due to Beddard *et al.* (1981) is illustrated in Fig. 1.24. The method relies upon the generation in the anisotropic crystal of a signal of frequency ω_3, the sum frequency of fluorescence ω_2 and laser pulse, ω_1. ω_3 can be distinguished spatially and in frequency, and by delaying the interrogating laser pulse in time, a profile of fluorescence decay can be built up.

The instantaneous power of the sum frequency in a crystal of length L is given by

$$P_\omega(L) \approx L^2 P_1 P_2 \frac{\omega_3}{\omega_1}, \tag{1.64}$$

where the subscripts 1, 2 and 3 refer to the gating pulse, the fluorescence and the sum frequency (given by $\omega_3 = \omega_2 \pm \omega_1$), respectively. By appropriate phase matching the difference frequency can be generated which can be used to measure fluorescence in the ultra-violet.

The fluorescence intensity I_s generated by the exciting pulse has a time profile given by

$$I_s(t) = \int_{-\infty}^{t} I_f(t')L(t-t')\,dt', \tag{1.65}$$

where t' is the time delay, $L(t)$ is the laser pulse shape and $I_f(t)$ is the molecular fluorescence intensity at time t. The signal $S(t)$ after passage through the crystal is given by

$$S(t) = \int_{-\infty}^{\infty} I_s(t')L(t-t')\,dt', \tag{1.66}$$

which combined with Equation 1.65 gives

$$S(t) = \int_{-\infty}^{t} I_f(t')A(t-t')\,dt', \tag{1.67}$$

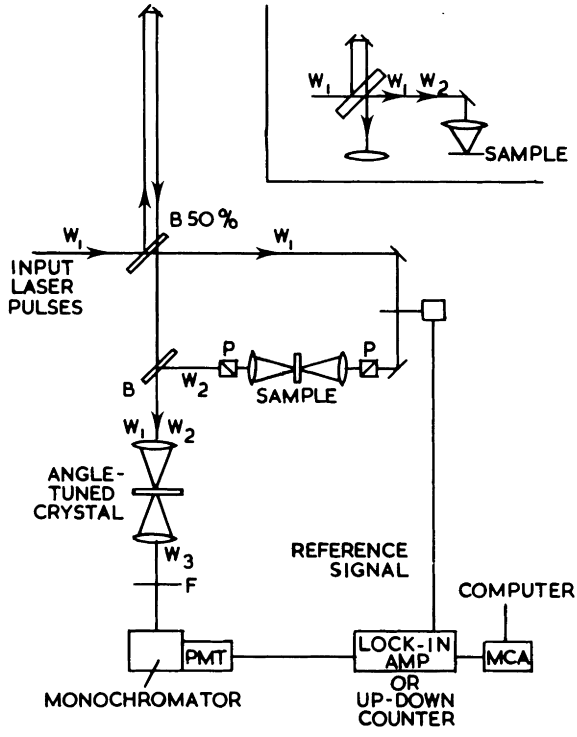

Figure 1.24 Experimental arrangements for time-resolved fluorescence up-conversion: F, filters; P, polarizers; C, a sectored disc chopper connected to a lock-in amplifier or photon counter; W_1, laser beam; W_2, fluorescence. The crystal is $LiIO_3$ (path length, 1 nm). The sample is contained in a glass cell of path length 1 nm mounted perpendicularly to the exciting beam and spun about an axis parallel to the beam, and the fluorescence is collected from the front face of the cell along the exciting beam axis. In an alternative method (inset) the sample is flowed through a cell or pumped through a nozzle to form a jet, and fluorescence is collected at 180° to the exciting beam. (After Beddard *et al.*, 1981.)

where $A(t)$ is the measured autocorrelation function of the laser pulse. As the autocorrelation function is readily measured, the signal can be fitted to the desired decay function at the shortest times with no *a priori* knowledge of the laser pulse shape. This offers a significant advantage over transient absorption methods where it is necessary to make assumptions about the laser pulse shape to facilitate curve fitting. When used to measure fluorescence decays, it offers several advantages over time-correlated single photon counting. As well as greatly improved time resolution, it is possible to detect fluorescence in the far red and infra-red without using special red-sensitive photomultipliers; for example fluorescence at 900 nm can be mixed with laser light

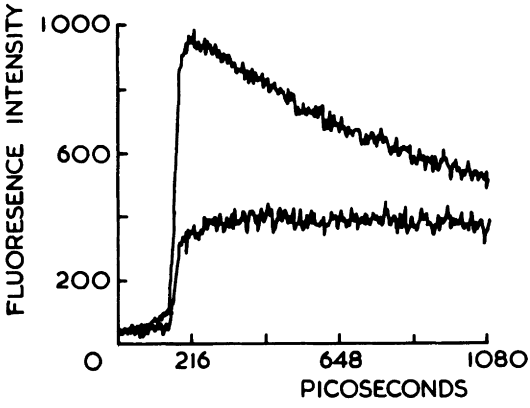

Figure 1.25 $I_{||}$ (upper), and $I_{\perp}$, (lower) curves for fluorophore rotating in alcohol solvent, up-conversion experiment (after Beddard *et al.*, 1981).

at 600 nm to generate a sum frequency at 360 nm. This advantage, however, bestows necessarily a corresponding disadvantage; that is up-conversion of fluorescence towards the blue end of the spectrum is rendered difficult owing to the absence of efficient crystals operating in the far ultra-violet.

The method can easily be adapted to make measurements of fluorescence anisotropy, and the quality of data produced is exemplified by Fig. 1.25. The precision of decay times measured using this arrangement is set by the optical delay time, which for convenience is of the order of 1 ps or less. The lower limit is set by the excitation pulse profile, which with present generation lasers is about 2 ps.

References

Badea, M. G. and Brand, L. (1979). *Meth. Enzymol.*, **61**, 378–425.
Beddard, G. S., Carlin, S., Harris, L., Porter, G. and Tredwell, G. S. (1978). *Photochem. Photobiol.* **27**, 433–438.
Beddard, G. S., Doust, T. and Porter, G. (1981). *Chem. Phys.* **61**, 17–23.
Beavan, S. W., Hargreaves, J. S. and Phillips, D. (1979). *Adv. Photochem.* **11**, 207–303.
Birks, J. B. (1970). "Photophysics of Aromatic Molecules", pp. 301–305. Wiley-Interscience, New York.
Birks, J. B. and Munro, J. H. (1967). *Prog. Reac. Kinet.* **4**, 239–303.
Blatt, E., Treloar, E. F., Ghiggino, K. P. and Gilbert, R. G. (1981). *J. Phys. Chem.* **85**, 2810–2813.
Cossins, A. R. (1981). In "Fluorescent Probes" (Beddard, G. S. and West, M. A., eds), pp. 39–80. Academic Press, London.
Forster, Th. (1946). *Naturwiss.* **33**, 166–171.

Ghiggino, K. P., Roberts, A. J. and Phillips, D. (1980). *J. Phys. E.* **13**, 446–449.
Gugger, H. and Calzaferri, G. (1980). *J. Photochem.* **13**, 295–307.
Hieftje, G. M., Haugen, G. R. and Ramsey, J. M. (1977). *Appl. Phys. Lett.* **30**, 463–465.
Hirayama, S. and Phillips, D. (1980). *J. Photochem.* **12**, 139–146.
Isenberg, J. (1975). In "Biochemical Fluorescence Concepts", Vol. 1 (Chen, R. F. and Edelhoch, H., eds) pp. 43–77. Marcel-Dekker, New York.
Knight, A. E. W. and Selinger, B. K. (1973). *Aust. J. Chem.* **26**, 1–27.
Koechlin, Y. (1961). Thesis, passim. University of Paris.
Meech, S. R. (1983). Thesis. University of Southampton.
Meech, S. R., O'Connor, D., Phillips, D. and Lee, A. G. (1983). *J. Chem. Soc. Faraday Trans. II*, **79**, 1563–1584.
Meserve, E. J. (1971). In "Excited States of Proteins and Nucleic Acids" (Steiner, R. F. and Weinryb, J., eds) p. 57. Plenum, New York.
Nemzek, T. L. and Ware, W. R. (1975). *J. Chem. Phys.* **62**, 477–489.
North, A. M. and Soutar, I. (1972). *J. Chem. Soc. Faraday Trans. II* **68**, 1101–1106.
O'Connor, D. V., Chewter, L. A. and Phillips, D. (1982). *J. Phys. Chem.* **86**, 3400–3404.
Palmer, T. F., Cehelnik, E. D., Cundall, R. B. and Lockwood, J. R. (1974). *J. Chem. Soc. Faraday Trans. II* **70**, 244–252.
Parker, C. A. and Hatchard, V. (1963). *Trans. Faraday Soc.* **59**, 284–290.
Phillips, D., Ghiggino, K. P. and Lee, A. G. (1979). In "Synchrotron Radiation Applied to Biophysical and Biochemical Research" (Castellani, A. and Quercia, U. F., eds) pp. 171–182. Plenum, New York.
Porter, G., Reid, E. S. and Tredwell, C. J. (1974). *Chem. Phys. Lett.* **29**, 469–472.
Poultney, S. K. (1972). *Adv. Elect. Elect. Phys.* **31**, 39–117.
Roberts, A. J., O'Connor, D. V. and Phillips, D. (1981). *Ann. N.Y. Acad. Sci.* **366**, 109–124.
Sakurovs, R. and Ghiggino, K. P. (1982). *J. Photochem.* **18**, 1–8.
Spears, K. G. and Rice, S. A. (1971). *J. Chem. Phys.* **55**, 5561–5581.
Strickler, S. J. and Berg, R. A. (1962). *J. Chem. Phys.* **37**, 814–822.
Ware, W. R. (1971). In "Creation and Detection of the Excited State", Vol. 1A (Lamola, A. A., ed.) pp. 213–326. Marcel-Dekker, New York.
Winkworth, A. C., Osborne, A. D. and Porter, G. (1982). In "Picosecond Phenomena III" (Eisenthal, K. B., Hochstrasser, R. M., Kaiser, W. and Lauterean, A., eds) p. 228. Springer-Verlag, Berlin.
Yguerabide, J. (1972). *Meth. Enzymol.* **26**, 498–578.